A Realtime Micro-Doppler Detection, Tracking and Classification System for the 94 GHz FMCW Radar System DUSIM

René Petervari[1], Fabio Giovanneschi[2], Winfried Johannes[3], María González-Huici[4]
Fraunhofer Institute for High Frequency Physics and Radar Techniques (FHR)
Wachtberg, Germany
E-Mail: {[1]rene.petervari,[2]fabio.giovanneschi,[3]winfried.johannes,[4]maria.gonzalez}@fhr.fraunhofer.de

***Abstract*— In the field of non-cooperative target classification micro-Doppler signatures provide valuable information on a diverse set of targets. In the recent years numerous applications were proposed in areas like road safety or infrastructure protection. However, real-world environments are often challenging and put high demands on hardware and software likewise. Often, time, memory or the signal-to-clutter ratio turn out to be critical factors. In consideration of these circumstances a computationally efficient and memory saving detection, tracking and classification system for real-world FMCW radar data is proposed and verified experimentally.**

***Keywords*— radar signal processing, radar target tracking, automatic target recognition, micro-Doppler features.**

I. Introduction

In the recent years radar target classification using micro-Doppler features has attracted considerable attention in multiple research areas related to non-cooperative target recognition. Some of the central applications are perimeter protection [1], UAV observation [2] and traffic safety [3]. A popular approach for micro-Doppler based radar target classification is based on features generated by singular value decomposition (SVD) of processed target spectrograms [2] and has also been used in [4].

Most of these approaches, however, focus on single targets in well known environments. Therefore, they use continuous wave (CW) radar without range resolution. In many cases these conditions will not hold and a more sophisticated approach is desirable. A way for the radar to resolve targets at different ranges is to increase the bandwidth and therefore use frequency modulated continuous wave (FMCW) radar. To the best of the authors' knowledge, the work in [3] presents the first paper that makes use of this principle extensively for an automotive application. An additional, but crucial part of a FMCW based classification system in a multi target environment must be a tracking algorithm, which is included in [3]. Another important criterion for the application to real-world environments is realtime capability which is the focus of this paper and the main design criterion for the proposed system.

In the subsequent sections a processing system for a radar sensor, i.e. the 94 GHz DUSIM radar system, is presented which incorporates the popular spectrogram and SVD approach proposed in [2] and the idea of the FMCW tracking and classification system of [3] in realtime. Other than in [3] a PHD tracking and association filter is used. The main novelty of the current approach lies in the design focus on realtime applicability and environmental robustness. The description of the system and the first experimental results are presented in the next sections.

II. Algorithm Description

The proposed signal processing unit for the 94 GHz FMCW radar system DUSIM consists of two central parts: a continuously working spectrogram extraction mode and a clocked feature extraction and classification mode that is invoked only every Z cycles.

A. Continuous Mode

The continuous mode includes the basic detection and tracking algorithms required for extracting a target-related spectrogram which are presented in the following two sections. The flowchart in Fig. 1 illustrates the proposed architecture.

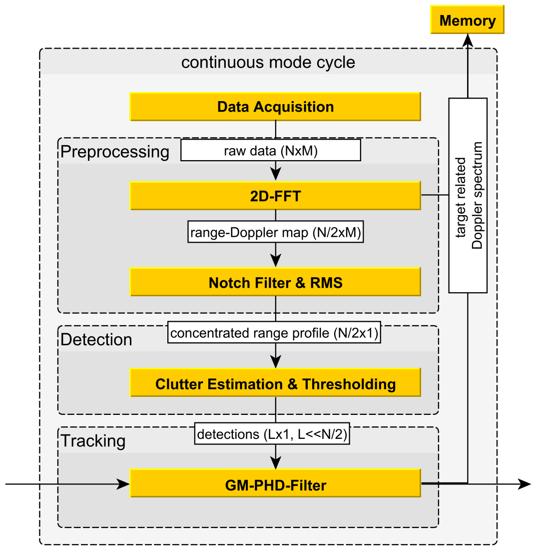

Fig. 1. The flowchart of a single processing cycle in the continuous mode.

1) Preprocessing

The input raw data comprises a sequence of M linear frequency modulation (LFM) waveforms, with N real-valued samples each, where N is even and M is a power of two. This data is transformed into a range-Doppler map using a two-dimensional Fourier transform. Continuing with the $N/2$ positive range bins and releasing the remaining memory for the next cycle, an exponential notch filter $\nu_{\sigma_\mathrm{w}}(f)$ given by

$$\nu_{\sigma_\mathrm{w}}(f) = 1 - \exp\left[-\frac{f^2}{\sigma_\mathrm{w}^2}\right] \qquad (1)$$

is applied to suppress the zero-Doppler component, where f denotes the Doppler frequency and σ_w the filter width. This filter is a modified version of the one used in [2]. It is followed by the calculation of the Root Mean Square (RMS) across the filtered Doppler domain in every range bin, which leads to a concentration of the remaining range-Doppler map into a single range profile.

2) Detection

In order to align this range profile to a constant background the range dependency of the clutter model was assumed to be $\propto R^2$ for windblown grass clutter. This dependency turned out to be suitable for the experimental setup (section III-A). Furthermore, it can be justified by the consideration that the illuminated area at range R is $\propto R^2$ since for grass it approximates a section of a sphere and by assuming a uniform reflectivity of grass, the radar cross section σ_RCS will also follow this trend. According to the radar equation the Signal-to-Noise Ratio (SNR) will obey

$$\mathrm{SNR} \propto \frac{\sigma_\mathrm{RCS}(R)}{R^4} \propto R^{-2}. \qquad (2)$$

As the SNR is an energy measure, the amplitude will be $\propto R$ and alignment is obtained by multiplying the concentrated range profile with R.

Given the aligned range profile, the cycle specific (uniform) clutter distribution in logarithmic scale is estimated by first determining the median. Then, the standard deviation σ_STD of the union of the signal below the median and a copy of this signal mirrored at the median is calculated. Assuming that this clutter background follows a Gaussian distribution in logarithmic scale, the threshold measured in terms of σ_STD above the median is directly related to the probability of false alarm p_fa given by the Standard Normal Distribution. For further reduction of detections, thus minimizing the load on the tracker, only the local maxima of a bunch of neighboured threshold excesses are counted as detections.

3) Tracking

In the scope of the present signal processing unit a Gaussian Mixture Probability Hypothesis Density (GM-PHD) filter [5] serves as tracking filter. It presents an alternative to the standard combination of a Kalman filter and a Joint Probabilistic Data Association (JPDA) filter used in [3]. For the sake of simplicity the GM-PHD filter uses a constant velocity approach which is suitable unless the track update rate (i.e. the cycle rate) is not too low to capture the target dynamics.

As indicated in Fig.1 the GM-PHD filter takes the current detections and the previous multi target state as inputs and calculates from these a new multi target state for the current cycle. Due to the constant velocity model the multi target states only constist of the range, the velocity and the track identification number (track ID) of each element in the set of current track hypotheses. According to [5] a hypothesis is considered as a confirmed track if its weight exceeds a threshold of 0.5 because the PHD represents the target density in the multistate space.

4) Spectrogram extraction

The extracted confirmed target states are now used to generate the corresponding Doppler spectra from the already calculated range-Doppler map at the respective target range. Finally, the confirmed target states and the corresponding Doppler spectra of the current cycle are saved together in the memory.

B. Clocked Mode

After Z cycles in continuous mode a single cycle in the clocked mode is evoked to classify the targets based on the spectrogram stored in the memory during these Z cycles. A cycle consists mainly of a feature extraction unit and a Support Vector Machine (SVM) based classifier analogous to the approach for continuous wave radar presented in [6].

1) Feature Extraction

The inputs of the SVM based classifier are obtained from the Principal Component Analysis (PCA) of the spectrograms with aligned main-Doppler. Therefore, the period of the clocked mode is adapted to the dynamic of the target's center-of-mass motion, such that it is long enough to extract meaningful micro-Doppler signatures but short enough to approximate the motion legitimately by a straight line. For larger creatures like humans, dogs or birds two seconds appear reasonable.

First, a second zero-Doppler notch filter like in paragraph II-A1 is applied to suppress the static background Doppler. Due to acceleration and non-zero velocity, which is present in many situations, the spectrograms are usually not aligned with the zero Doppler axis ($d = 0$). To align the spectrogram $S(d_j, t_i)$ to a set of straight lines $g_n(t_i)$ (i.e. a fan) with equally spaced inclination angles is created; hence covering the whole possible range of linear Doppler evolution. To avoid computationally expensive interpolation these lines are rounded to integers and become step functions. The spectrogram is then aligned to every element $g_n(t_i)$ of the fan of straight lines and the RMS in temporal direction t is calculated and added up to a single value δ

$$\delta = \sum_{j=1}^{J} \mathrm{RMS}\left[S(d_j - g_n(t), t)\right]. \qquad (3)$$

The smallest value of δ indicates the best alignment. After aligning the spectrogram using δ the remaining offset to the zero Doppler axis is corrected by determining the Doppler bin ϵ with maximum energy

$$\epsilon = \arg \max_{d} \sum_{i=1}^{I} \left[S(d_j - g_n(t), t) \right]^2 . \quad (4)$$

The final spectrogram is given by $S(d_j - g_n(t) - \epsilon, t)$. Fig. 2 shows the aligned spectrogram extracted of a tracked target.

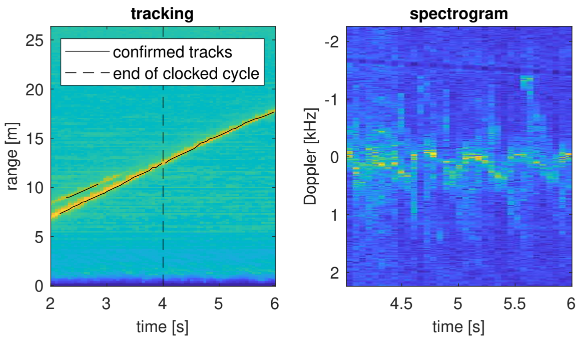

Fig. 2. The confirmed track and the corresponding spectrogram.

From the aligned spectrogram the principal components in temporal direction are calculated using a SVD approach. We apply the SVD as a matrix factorization method to decompose the resulting aligned spectrograms $\mathbf{S}$ into three different matrices: singular value matrix $\mathbf{\Lambda}$, left singular vectors $\mathbf{U}$ and right singular vectors $\mathbf{V}$. The original spectrogram $\mathbf{S}$ can be reconstructed as follows: $\mathbf{X} = \mathbf{U}\mathbf{\Lambda}\mathbf{V}'$. The left singular vectors $\mathbf{U}$ (which represent the eigenvectors of the spectrogram auto-correlation matrix) are used to create an orthogonal set of features for classification.

In our case, we checked that the first 6 singular vectors were sufficient to reconstruct the spectrograms while the remaining ones were mostly responsible for noise contributions. To obtain features with high "energy compaction" [2], we calculated the Fourier transform of these singular vectors, which allows to see where most of the signal information in the eigenvectors is concentrated. The final feature vector which is used for classification is obtained by stacking together the 6 transformed singular vectors.

2) Classification

The generated feature vectors are now classified using a pre-trained SVM. Given a manually pre-defined collection of labelled observations, i.e. feature vectors, the SVM searches for a functional $f : \mathbb{R}^n \rightarrow \mathbb{R}$ that maps any given observation $\mathbf{x}_i$ to a class $c \in \mathbb{R}$. The kernel function that is used here to compute the high dimensional operations in the feature space, is the Gaussian Radial Basis Function (RBF): $\kappa(\mathbf{x}_i, \mathbf{x}_j) = \exp(-\gamma(||\mathbf{x}_i - \mathbf{x}_j||)^2 + C)$, where $\gamma > 0$ is the free parameter that determines the influence of the support data vector $\mathbf{x}_j$ on the class of the vector $\mathbf{x}_i$ in the original space and C is the parameter for the soft margin cost function, which controls the influence of each individual support vector [7]. To optimally select the SVM input parameters, we arrange the original classification set into training and validation vectors in ν different ways (ν-fold cross-validation with ν=5) to arrive at a certain mean cross-classification accuracy of the validation vectors. For more details of SVM, we refer the reader to [7].

III. Experimental Validation

The proposed detection, tracking and classification system was tested and validated on experimental data acquired by the DUSIM radar system.

A. Radar System and Experimental Setup

The four-channel 94 GHz radar system DUSIM [8], named after the corresponding research project "Dual Use Sensor for Mid-Range Applications", was developed for active protection aiming at a target distance between 8 m and 250 m. It operates a frequency modulated continuous wave signal (FMCW) with a bandwidth of approximately 1 GHz at an emission power of 100 mW. In the scope of the development the sensor was tested under realistic conditions in several measurements where it proved to detect flying projectiles and other ammunitions.

A common task for automatic target recognition systems in short range is the detection and interpretation of human motion. Using this setting as a benchmark for the presented system, a pedestrian was measured at two different velocities (walking, running) in the four complementary directions (from left to right, from right to left, approaching and walking away) with respect to the radar's position. Each case was repeated five times to create an acceptable amount of training and test data.

B. Algorithm Performance

1) Computation Time

Table 1. Computation time on the experimental data set.

Cycle Code	**Computation Time**		
	min [ms]	**max [ms]**	**mean [ms]**
continuous	0.21	14.42	0.45
clocked	0.47	300.95	67.56

The proposed algorithm was implemented offline on a desktop PC (Intel® Xeon® CPU E5-1640 v4 @ 3.5 GHz; 32 GB RAM) in C++. With $Z_{\text{chirps}} = 256$ waveforms acquired during every cycle in continuous mode. For all test sets, which consisted in data acquired in ca. two hours of measurements, the application runs in realtime. This means that the processing in the continuous mode consumes less time than the acquisition of the Z_{chirps} waveforms. At a pulse repetition frequency (PRF) of 4.5 kHz the acquisition in continuous mode lasts approximately 56.9 ms, whereas the processing of an average continuous cycle for a single target lasts 0.45 ms (see Table 1) and 14.42 ms at maximum. To avoid affecting the acquisition by possibly longer processing times and thereby missing incoming data, the continuous cycle processing was implemented parallel to the acquisition with a double buffer concept. Due to the longer duration of the processing during the clocked cycle, another double buffer to hold the spectrograms and tracks was used. The current implementation uses three CPU cores, however, the parallel processing and the double buffers can be discarded so the system can work on a single core with half of the memory; this at the expense of a lowered temporal resolution in the spectrograms.

2) Memory

Beneath the computation time, required memory plays an important role in commercial realtime applications. In continuous mode the present approach mostly requires memory to store the actual and the previous range-Doppler map (double buffer concept). Before the clocked memory buffer (holding the spectrogram and tracking data) is overwritten with new data, the data is stored in a second clocked memory buffer to assemble the spectrograms and maintain the tracking during the processing of the data in the first buffer.

Table 2. Main memory sizes for the parallel processing concept.

memory	size	type
continuous	$2Z_{\text{chirps}}N$	float
clocked	$2\,(ZZ_{\text{chirps}}J_{\max} + J_{\max}J_{\max})$	complex float

The required memory of the present system is listed in Table 2. The major design parameters are the number of evaluated real samples ($N = 352$) and the number of waveforms ($Z_{\text{chirps}} = 256$) acquired during a single cycle in the continuous mode. Additionally, the maximum number of expected targets ($J_{\max} = 40$) and the number of cycles in the clocked mode ($Z = 35 \approx 2$ s) are important measures for the size of the clocked cycle memory. Both control the maximum size of the stored spectrograms and tracking states.

C. Classification Results

Table 3. Confusion matrix for SVM classification
(r = run, w = walk, lat. = lateral, adv. = advancing, rec. = receding).

in %	**lat./w**	**lat./r**	**adv./w**	**adv./r**	**rec./w**	**rec./r**
lat./w	96.36	1.82	1.82	0	0	0
lat./r	8.33	91.66	0	0	0	0
adv./w	0	0	94.74	0	0	5.26
adv./r	0	0	21.43	78.57	0	0
rec./w	0	0	4.16	0	95.83	0
rec/r	0	0	0	0	0	100

To assess the performances of the SVM classifier (see section II-B2) we divided the entire dataset of FMCW measurements into a training set and a test set from which we respectively extracted 186 and 155 feature vectors associated to aligned spectrograms coming from confirmed tracks of six different classes of single pedestrians movements (see section II-B1 and II-B2). The parameters of the RBF kernel, selected after the five-fold cross-valdation, are $\gamma = 0$ and $C = 5$. Table 3 shows the classification accuracy of the test set. The confusion matrix shows that the proposed classification approach can successfully discriminate between moving directions and two different paces of a single pedestrian. This is a remarkable result considering the amount of unwanted contributions present in this measurement campaign (generated from wind, rain, antenna cross-talk, etc.). This is also another indicator of the quality of the GM-PHD filtering and spectrogram alignment procedures. The drop in accuracy for the advancing/running case, is mostly dependent on the modest number of feature vectors for that class (17 for training and 14 for test). Future works may include a larger dataset with more classes (i.e. groups, cyclist, etc.).

IV. Conclusion

In the scope of this paper a detection, tracking and classification system is presented, which is designed for real-world multi target scenarios. Beneath the requirement of spatial resolution, high classification confidence, real-world applications require realtime applicability. When testing our system with a pedestrian target in a wet, windblown grass clutter as benchmark test, the algorithm proved to be efficient in terms of the use of computation power and memory. High classification rates could be reached in the discrimination between walk and run each in tangential and longitudinal movement with respect to the radar. Further performance improvement is expected by additional testing and training data.

Acknowledgement

Finally, the authors wish to thank Dr. Michael Caris for the kind opportunity to use the DUSIM radar system and Volker Port for the competent operation and his helpful assistance during the experimental works.

References

[1] S. Björklund, T. Johansson, and H. Petersson, "Target classification in perimeter protection with a micro-Doppler radar," in *Radar Symposium (IRS), 2016 17th International*. IEEE, 2016, pp. 1–5.

[2] P. Molchanov, "Radar target classification by micro-Doppler contributions," *Tampereen teknillinen yliopisto. Julkaisu-Tampere University of Technology. Publication; 1255*, p. 142, 2014.

[3] T. Wagner, R. Feger, and A. Stelzer, "Radar signal processing for jointly estimating tracks and micro-Doppler signatures," *IEEE Access*, vol. 5, pp. 1220–1238, 2017.

[4] F. Fioranelli, M. Ritchie, and H. Griffiths, "Classification of unarmed/armed personnel using the NetRAD multistatic radar for Micro-Doppler and Singular Value Decomposition features," *IEEE Geoscience and Remote Sensing Letters*, vol. 12, no. 9, pp. 1933–1937, Sep. 2015.

[5] B.-N. Vo and W.-K. Ma, "The Gaussian mixture probability hypothesis density filter," *IEEE Transactions on signal processing*, vol. 54, no. 11, p. 4091, 2006.

[6] P. Molchanov, K. Egiazarian, J. Astola, R. I. A. Harmanny, and J. J. M. de Wit, "Classification of small UAVs and birds by micro-Doppler signatures," in *2013 European Radar Conference*, Oct 2013, pp. 172–175.

[7] C.-C. Chang and C.-J. Lin, "LIBSVM: a library for support vector machines," *ACM transactions on intelligent systems and technology (TIST)*, vol. 2, no. 3, p. 27, 2011.

[8] M. Caris, "DUSIM - A mmW sensor to trigger active indicrect protection measures," in *Internationales Symposium Indirekter Schutz (ISIP)*, 2018.